

# Image-Based Penetration Monitoring of CO<sub>2</sub> Laser Beam Welding

*Characteristics of the weld pool and plasma plume as viewed through a dual-camera system indicate degrees of weld joint penetration*

BY R. K. HOLBERT, R. W. RICHARDSON, D. F. FARSON AND C. E. ALBRIGHT

**ABSTRACT.** A dual-camera video system was developed to provide real-time information about the penetration modes of CO<sub>2</sub> laser beam welding for process quality monitoring and control. An experiment was designed to vary the penetration modes during welding by continuously changing the focal point position at different power levels and travel speeds. A study of the video images of the weld pool/keyhole region identified three types of weld pools: flat, depressed and keyhole. Images of the plasma plume revealed that a wispy, diverging fantail-shaped plume corresponded to the steady-state, flat and weakly depressed weld pools. As the power density and weld penetration depth increased, the diverging fantail plume changed to a concentrated columnar shape. A keyhole cavity was initiated when the diameter of the base of the columnar plume at the coupling spot (beam/material interaction site) and the calculated beam spot size were identical. Video images of the events during transition into and out of the keyhole mode from two vantage points were studied to identify features indicative of the presence of a keyhole. Keyhole welds were associated with a very intense columnar plume, elevated weld pool rim and several other visual cues. The unique perspective produced by the dual-camera video system could provide the basis for an in-process penetration control strategy and add to under-

standing of the physical processes that affect laser welding penetration mode and pool/plume dynamics during CO<sub>2</sub> laser welding.

## Introduction

An important feature of continuous-wave, carbon dioxide (CO<sub>2</sub>) laser welding is the ability to vary power density on the material surface over wide ranges by varying beam focus and power. Focusing the beam to a very small, high-power-density spot leads to the formation of a vapor cavity and a deep, narrow "keyhole-mode" weld. The high travel speeds and low thermal distortion associated with this welding mode give keyhole laser welding important advantages over other welding processes in certain applications. On the other hand, shallow conduction-mode laser welds generated at lower power densities are advantageous for surfacing applications where minimal penetration is usually desired.

The welding mode and the weld penetration depth in either mode are deter-

mined primarily by power density at the material surface, travel speed, base material properties and gas shielding. Since a number of these process inputs are susceptible to variation, process monitoring and feedback control to ensure proper welding penetration would be beneficial. In-process measurement of the laser welding mode (whether keyhole or conduction) and penetration depth is currently not possible, but it is vital for successful monitoring and control implementation. These measurements are difficult because of the small size of the laser weld, the harsh environment (smoke, spatter, high temperatures, etc.) and the practical need to make measurements from the topside of the work. Thus, developments in welding mode and penetration depth measurement are critical to the improvement and increased application of in-process laser weld monitoring and control capability. In this investigation, real-time images of the weld pool, keyhole and plume are analyzed to determine what weld mode and penetration information can be extracted from them.

## Laser Weld Penetration Monitoring

Techniques that provide direct in-process measurements of laser weld penetration (such as X-ray or ultrasonic sensing) have not been developed to the point that they are generically practical for industrial use. Thus, a popular approach (and the approach taken in this work) is to make measurements of other welding process information that is related to penetration and then infer the state of penetration from these measurements. Past work has been directed at analysis of

### KEY WORDS

Keyhole Mode  
CO<sub>2</sub> Laser  
Camera System  
Monitoring  
Conduction Mode  
Weld Penetration

R. K. HOLBERT is with Siemens Westinghouse Power Corp., Orlando, Fla. R. W. RICHARDSON, D. F. FARSON and C. E. ALBRIGHT are with The Ohio State University Department of Industrial, Welding and Systems Engineering, Columbus, Ohio.



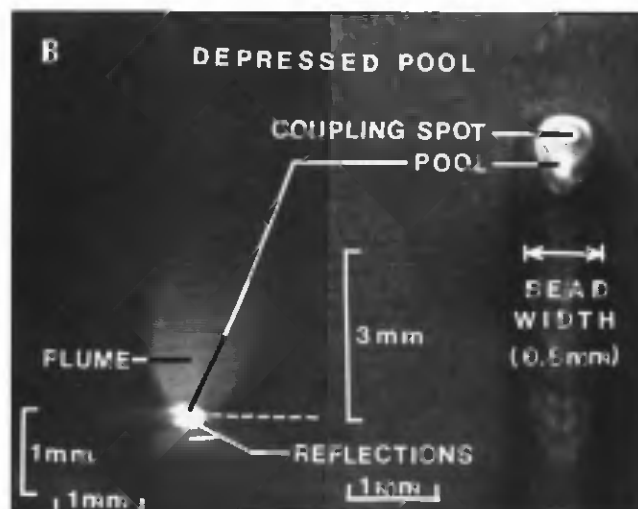
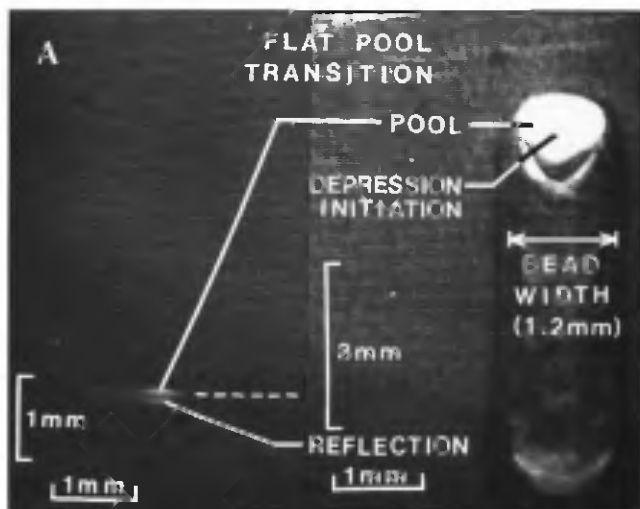


Fig. 3 — Transition from a flat weld pool to a depressed weld pool from a 1.5-kW test weld (2.03 m/min). A — Flat pool image; B — depressed pool image.

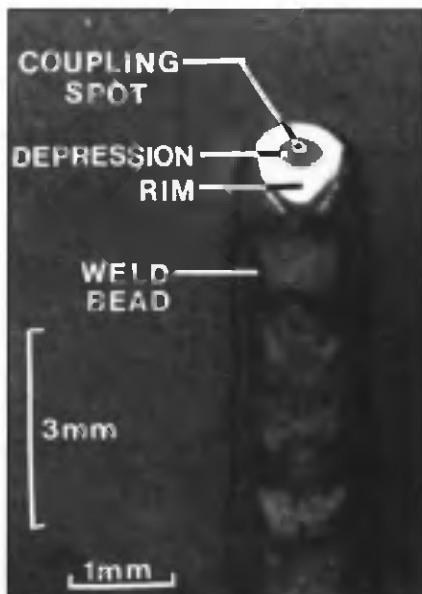


Fig. 4 — Inclined-camera image of a depressed pool from a 1.5-kW test weld (2.03 m/min) showing the coupling spot, the depression and the pool rim.

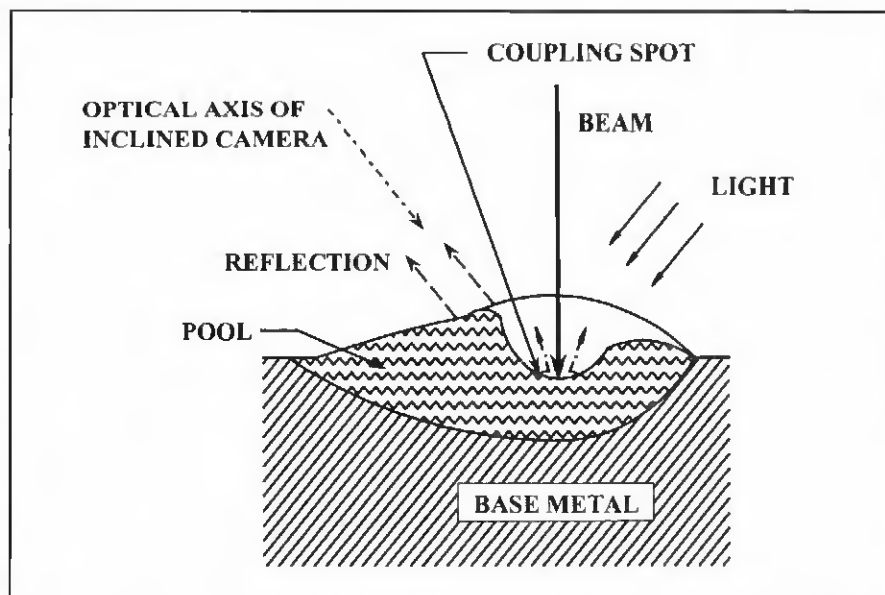


Fig. 5 — Depressed weld pool characteristics.

mode transitions from the video images. Recorded video images captured the dynamic behavior of the plasma and weld pool with power density change and resulting mode transition along the weld.

#### Video System

The video system recorded images from two camera systems (including CCD cameras, long-distance microscopic lenses and optical filters) and displayed them on a split monitor screen for simultaneous viewing of the weld

process from two angles to facilitate analysis. Images from an inclined camera (mounted above and behind the weld at 45 deg to the beam axis in the direction of weld motion, as illustrated in Fig. 1) primarily provided information about pool characteristics, while images from a horizontal camera (mounted transverse to the direction of motion, as illustrated in Fig. 1) contained information about the plasma plume.

Both cameras used long-distance microscopic lenses with an approximate working distance of 305 mm. The cam-

era/lens combination allowed a microscopic observation from a safe distance, protecting the camera and lens from smoke and spatter emitted by the weld. The shutter speed of the inclined camera was  $\frac{1}{1000}$  s and that of the horizontal camera was  $\frac{1}{2000}$  s. The video frame rate was fixed for both cameras at 30 interlaced frames/s. Quartz projector lamps of 300 W were used to overpower the plasma and thermal emissions so the weld pool could be observed clearly. One lamp was placed above the horizontal camera to illuminate the sample's surface, as shown







when the plume was visibly present.

In the depressed-pool images from both cameras, the features of primary interest are the plume, pool and coupling spot. Observations of the plume could be made from the horizontal and inclined images. The pool was also identifiable in both camera images, but the coupling spot was visible only in the inclined-camera images. The depressed pool appeared to be concave at the CO<sub>2</sub> laser beam/material interaction location. This observation agrees with the conclusions of Voelkel and Mazumder (Ref. 7) based on their video images of conduction-mode welds. Three regions of the depressed pool were identified in the inclined-camera images: the rim, the depression and the coupling spot. Figure 4 shows the coupling spot in the upper portion of the depressed pool surrounded by a dark band and then a very bright outer ring (teardrop shaped) in the inclined-camera image of a 1.5-kW test weld. The bright outer ring is interpreted to be the flat, tranquil upper rim of the pool, projecting above the sample's surface. Where the inclination angle of the depression walls is unfavorable for light reflection into the camera, a dark band can be seen in the pool. A bright nucleus is evident at the center of this dark depression. This bright spot is identified as the coupling spot and is accentuated in the darkness of the depression in the inclined-camera images.

Based on video images of depressed pools, the illustration in Fig. 5 depicts the depressed pool relative to the laser beam, the high-intensity lighting and the optical axis of the inclined camera. The outer portion of the molten pool forms a rim around the shallow depression, which is in the interior of the pool located near the leading edge. Since the coupling spot is at the center of the depression, the depression and coupling spot are apparently centered on the beam axis. This observation agrees with the findings of Voelkel and Mazumder (Ref. 7). Illumination of the rim is by the auxiliary lighting opposite the inclined camera. This light is specularly reflected toward the inclined camera, but the walls of the depression are not at the appropriate angle for reflection. Thus, the depression appears dark in the images with the bright coupling spot in the center. Figure 5 shows the highest location on the rim is on either side of the depression where the Y-Z plane passes through the beam axis. The center of the coupling spot and the lowest point in the depression occur at the intersection of the beam axis and this Y-Z plane. It appears that this location on the rim is composed of the displaced molten metal

from the depression in the pool.

Figure 6 shows six successive (but noncontiguous) horizontal-camera images of the plume transformation over the depressed pool for a 1.5-kW test weld with a travel speed of 2.03 m/min. During the time spanned by the six images, the focal point position approached the surface from an elevation of +10 mm (above the surface) in the first image to +4 mm in the last image. There was no plume present in the first image when the pool initially changed from the flat pool to a depressed pool. A slightly crowned appearance of the pool is the only indication the pool was not completely flat.

The focal point position was closer to the surface in the second image, and the increased power density resulted in the formation of a weak, wispy, fantail-shaped plume over the depressed pool. In the third and fourth images, the fantail plume developed into a more distinct vapor cloud and began to increase in height as the spot size became continuously smaller. Finally, the fantail plume concentrated into a columnar shape, as seen in the fifth image. The sixth image shows the weld just before initiation of the keyhole cavity, when the beam waist was 4.0 mm above the material surface. The columnar plume was more slender and slightly taller than in the previous images. No significant change was observed in the diameter of the coupling spot throughout the sequence, even though the beam spot size and the width of the plume base decreased.

During the image sequence shown in Fig. 6, cross section measurements (repeated for two welds with the same parameters) revealed the weld pool penetration increased from 0.38 mm to 0.52 mm. Thus, the plume shape (divergence angle) and height are both observables that could correlate to power density and weld depth in conduction-mode welds. Additional tests are required to quantify the relationship and determine the accuracy of penetration estimates obtained from plume-shape measurements.

Comparing the sizes of the various features in the conduction-mode weld images, a relationship that consistently predicted the transition to or from keyhole-mode welding was noted. Figure 7 summarizes this result. The figure plots the dimensions of three features measured in a sequence of images taken as a weld transitioned from keyhole to depressed mode when the focal position moved from -4.4 to -7.3. Prior to the welding mode transition, the coupling spot diameter, estimated beam spot diameter and plume base diameter were all approximately equal. This relationship is

potentially useful in determining when a weld is about to switch in or out of keyhole mode.

## Comparison of Keyhole- and Conduction-Mode Weld Images

Image observables that are potentially useful for detecting keyhole weld formation were determined by studying pictures taken just before and after the transition to and from keyhole welding. Figure 8 shows one video image taken just at the instant of the depressed-to-keyhole transition and another a few video frames later. Figure 9 shows weld cross photographs corresponding to the plume images in Fig. 8. A columnar plume is evident in the horizontal-camera image and is representative of the depressed pool prior to the keyhole cavity formation. However, an intense glow denotes a keyhole plume was beginning to develop in the inclined-camera image. The weld cross section in Fig. 9A shows a very deeply depressed conduction mode weld pool. Images at the bottom of Fig. 8 show the keyhole pool and plume as they were beginning to stabilize. An extremely bright, dynamic keyhole-pool plume (in the horizontal-camera image) signified the formation of the keyhole cavity. Also, the pool height increased significantly during the stabilization of the keyhole cavity, appearing as a "rooster-tail" wake behind the coupling spot. This wake is presumably formed by displacement of the molten material from the keyhole cavity. It also causes turbulence in the molten pool resulting in the "ruffled" appearance. The bottom inclined-camera image in Fig. 8 shows that the pool widened dramatically and the pool shape changed from a small teardrop of the depressed pool to a large, uneven elongated ellipse of the keyhole pool. Keyhole initiation also resulted in the increase of the coupling spot dimensions. The corresponding keyhole-mode weld cross section in Fig. 9B confirms the dramatic increases in weld width and depth that were associated with the onset of keyholing.

In summary, both the plume shape and intensity, as well as the measured weld pool height, were clear indications of whether or not the weld was in keyhole mode. Pool width and surface appearance also appeared to be potentially useful for this purpose.

## Conclusions

The investigations using the video system and weld images led to the conclusions below.

